



HAL
open science

New observations of electromagnetic harmonic ELF emissions in the ionosphere by the DEMETER satellite during large magnetic storms

Michel Parrot, A. Buzzi, O. Santolík, Jean-Jacques Berthelier, J. A Sauvaud, J.-P. Lebreton

► **To cite this version:**

Michel Parrot, A. Buzzi, O. Santolík, Jean-Jacques Berthelier, J. A Sauvaud, et al.. New observations of electromagnetic harmonic ELF emissions in the ionosphere by the DEMETER satellite during large magnetic storms. *Journal of Geophysical Research*, 2006, 111 (A08301), 10.1029/2005JA011583 . insu-03037492

HAL Id: insu-03037492

<https://insu.hal.science/insu-03037492>

Submitted on 3 Dec 2020

HAL is a multi-disciplinary open access archive for the deposit and dissemination of scientific research documents, whether they are published or not. The documents may come from teaching and research institutions in France or abroad, or from public or private research centers.

L'archive ouverte pluridisciplinaire **HAL**, est destinée au dépôt et à la diffusion de documents scientifiques de niveau recherche, publiés ou non, émanant des établissements d'enseignement et de recherche français ou étrangers, des laboratoires publics ou privés.

New observations of electromagnetic harmonic ELF emissions in the ionosphere by the DEMETER satellite during large magnetic storms

M. Parrot,¹ A. Buzzi,¹ O. Santolík,² J. J. Berthelier,³ J. A. Sauvaud,⁴ and J. P. Lebreton⁵

Received 21 December 2005; revised 21 April 2006; accepted 27 April 2006; published 4 August 2006.

[1] DEMETER (Detection of Electro-Magnetic Emissions Transmitted from Earthquake Regions) is an ionospheric microsatellite launched on a polar orbit at an altitude of 710 km. Its scientific payload allows to measure electromagnetic waves and plasma parameters. During the strong magnetic storm from 8 to 10 November 2004, intense electromagnetic harmonic emissions between 500 and 2000 Hz have been detected at midlatitudes and similar emissions were also observed on 21–22 January 2005 and on 15 May 2005 during two magnetic storms of lower intensity. They can be observed on consecutive orbits, either in one hemisphere or in both hemispheres at the same L values. On the dynamic energy/time spectrograms that are available in the DEMETER survey modes these emissions appear most often as patches of intensified signals lasting a few tens to hundreds of seconds with a frequency structure showing nearly equally spaced frequency bands. Such a frequency structure could be explained if the waves originate from the generation of Electro-Magnetic Ion Cyclotron (EMIC) waves at proton cyclotron harmonics. When waveforms are available during burst modes, allowing a fine-resolution frequency analysis, these emissions appear in one orbit be composed of a set of lines slowly drifting in frequency with time. During periods with a high magnetically activity, the ionosphere and the magnetosphere are severely disturbed and these waves could be generated at relatively low L values and propagate from their equatorial source region along density gradients down to the altitude of the satellite. Energetic electron data obtained onboard DEMETER indicate that these waves interact with the energetic electron populations.

Citation: Parrot, M., A. Buzzi, O. Santolík, J. J. Berthelier, J. A. Sauvaud, and J. P. Lebreton (2006), New observations of electromagnetic harmonic ELF emissions in the ionosphere by the DEMETER satellite during large magnetic storms, *J. Geophys. Res.*, *111*, A08301, doi:10.1029/2005JA011583.

1. Introduction

[2] The paper is related to the description of electromagnetic harmonic emissions observed by the microsatellite DEMETER. These emissions are detected in the ELF range (500 Hz to 2 kHz) in the upper ionosphere during large magnetic storms, and it is shown that they could be related to Electro-Magnetic Ion Cyclotron (EMIC) waves. EMIC waves have been studied for a long time both by ground and satellite experiments. Initial observations by satellite were made by *Russell et al.* [1970], *Gurnett* [1976], and *Kintner and Gurnett* [1977]. EMIC waves have been seen in

association with intense electron fluxes on the auroral field lines with the S3-3 satellite [*Kintner et al.*, 1979; *Temerin and Lysak*, 1984], the Freja satellite [*Hamrin et al.*, 2002], the Fast satellite [*Chaston et al.*, 2002], and the Polar satellite [*Santolík et al.*, 2002b]. They have been also observed in the equatorial plane at various L values by the GEOS satellites [*Young et al.*, 1981], the Akebono satellite [*Sawada et al.*, 1991; *Kasahara et al.*, 1994; *Liu et al.*, 1994], the Equator-S satellite [*Mouikis et al.*, 2002], and the CRESS satellite [*Fraser and Nguyen*, 2001; *Meredith et al.*, 2003]. In this equatorial region, EMIC waves are generated from the ion cyclotron instability driven by the anisotropic distribution of ring current energetic ions during magnetic storms [see, e.g., *Mouikis et al.*, 2002; *Summers and Thorne*, 2003, and references therein]. They are characterized by harmonic structures with electric and magnetic field power between the first multiples of the proton cyclotron frequency. EMIC waves are known to take part in the precipitation of electrons [*Lorentzen et al.*, 2000; *Summers and Thorne*, 2003; *Meredith et al.*, 2003].

[3] Section 2 will briefly present the experiments onboard DEMETER. The events are described in section 3. Wave analysis of these events is shown in section 4. The possible

¹Laboratoire de Physique et Chimie de l'Environnement, CNRS, Orléans, France.

²Faculty of Mathematics and Physics, Charles University, Prague, Czech Republic.

³Observatoire de Saint Maur, Centre d'Etude des Environnements Terrestre et Planétaires, Saint Maur des Fossés, France.

⁴Centre d'Etude Spatiale des Rayonnements, CNRS, Toulouse, France.

⁵Research and Scientific Support Department, ESA/ESTEC, Noordwijk, Netherlands.

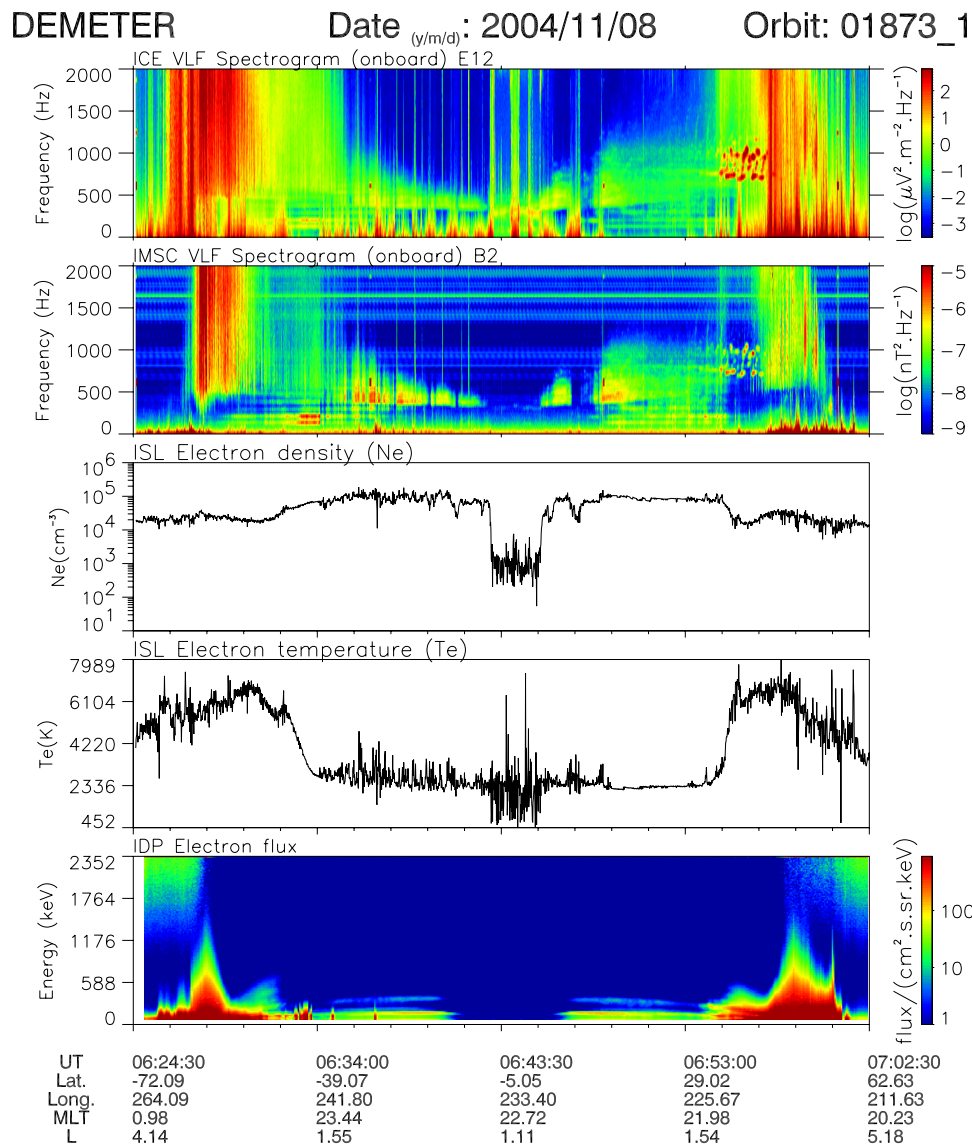


Figure 1. Data recorded during the up-going half-orbit 1873 on 8 November 2004. (top to bottom) VLF spectrogram of one electric component, VLF spectrogram of one magnetic component, electron density, electron temperature, and energetic electron flux. The data are displayed as function of the time in UT, the geographic latitude and longitude, the magnetic local time (MLT), and the L value.

origin of these emissions is discussed in section 5 whereas section 6 presents conclusions.

2. Wave and Plasma Experiments Onboard DEMETER

[4] The platform of DEMETER which was launched on 29 June 2004 is described by *Cussac et al.* [2006]. Its scientific payload is composed of several instruments which provide a nearly continuous survey of the plasma, waves and energetic particles around the Earth. The electric field experiment uses four electric probes to measure the three components of the electric field in a frequency range from DC up to 3.5 MHz. The search-coil magnetometer, measures the three components of the magnetic field in a frequency range from a few hertz up to 20 kHz. The Langmuir probe gives access to the electron density and

temperature. The thermal ion spectrometer measures the ion density, composition, temperature and flow velocity. A solid state energetic particle detector measures high energy electrons and protons looking in a direction perpendicular to the orbit plane, i.e., measuring particles with a mirror point in the vicinity of the satellite. Details about these experiments are given by *Berthelier et al.* [2006a, 2006b], *Lebreton et al.* [2006], *Parrot et al.* [2006], and *Sauvaud et al.* [2006]. There are two scientific modes: a survey mode where spectra of one electric and one magnetic component are onboard computed up to 20 kHz with a frequency resolution of 19.25 Hz, and a burst mode where waveforms of one electric and one magnetic components are recorded up to 20 kHz, and waveforms of the six electromagnetic field components are recorded up to 1.25 kHz. The burst mode which is triggered above predetermined regions allows performance of spectral analysis with better frequency

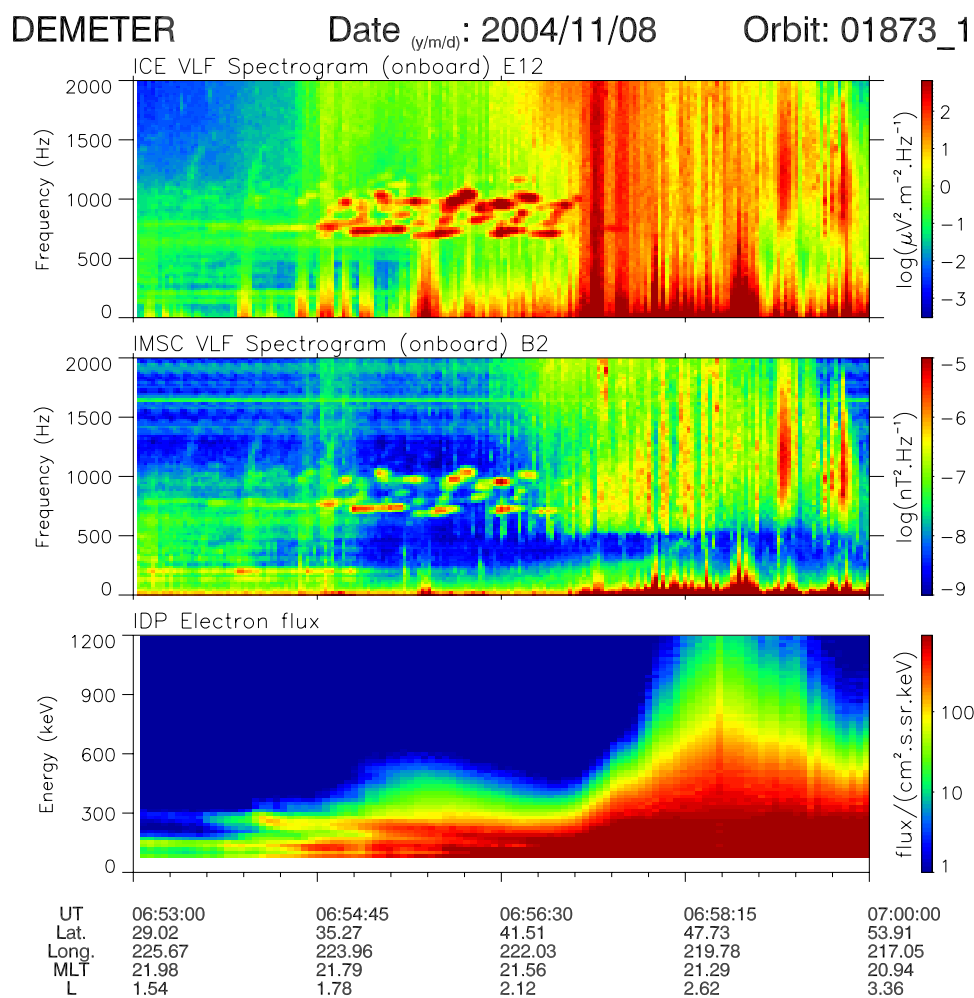


Figure 2. Zoom of Figure 1. (top to bottom) VLF spectrogram of one electric component, VLF spectrogram of one magnetic component, and energetic electron flux.

resolution and determination of the propagation characteristic of the waves. There is an onboard calibration at 625 Hz and 10 kHz which could be activated at each mode change and after every 4, 8 or 12 mn. DEMETER was launched on a polar and circular sun-synchronous orbit with an altitude of 710 km. Owing to technical reasons data are only recorded at invariant latitudes less than $\sim 65^\circ$. All data files and plots are organized by half-orbits [Lagoutte *et al.*, 2006]. The up-going half-orbits (invariant latitude between 65°S and 65°N) correspond to nighttime (2200 LT) and the down-going half-orbits (invariant latitude between 65°N and 65°S) to daytime (1000 LT).

3. The Events

[5] Data recorded during three different magnetic storms will be shown in chronological order. The first severe storm after the launch occurred on 8–10 November 2004 (maximum $Dst = -373$ nT and $K_p = 9$ on 8 November). The two others have been seen on 21–22 January 2005 (maximum $Dst = -105$ nT and $K_p = 8$) and on 15 May 2005 (maximum $Dst = -256$ nT and $K_p = 8$).

[6] Figure 1 shows data recorded during a complete half-orbit on 8 November 2004 between 0624:30 and 0702:30 UT (nighttime). The first and second panels display the spectrograms between 0 and 2 kHz of one electric and one magnetic component, respectively. The electric component is horizontal and perpendicular to the orbital plane. The third and fourth panels show the electron density and electron temperature obtained from the Langmuir probe, and the bottom panel represents an energy spectrogram (30–2352 keV) of the locally mirroring electrons. In the first and second panel a new type of electromagnetic emissions can be observed between 0654:45 and 0657:00 UT in a frequency band between 650 and 1180 Hz. During this time interval, the maximum intensities of the electric and magnetic spectrograms are $1.5 \times 10^4 \mu\text{V}^2 \text{m}^{-2} \text{Hz}^{-1}$ and $6.4 \times 10^{-6} \text{nT}^2 \text{Hz}^{-1}$, respectively. The other waves observed during this very disturbed period will not be discussed in this paper. A zoom is shown in Figure 2 which represents from the top to the bottom, the electric spectrogram, the magnetic spectrogram and energy-time spectrogram of electrons with a local pitch angle close to 85° . It is shown that the emission consists of patchy elements. Another example recorded on 9 November 2004 is shown in Figure 3 which is similar to Figure 1. The

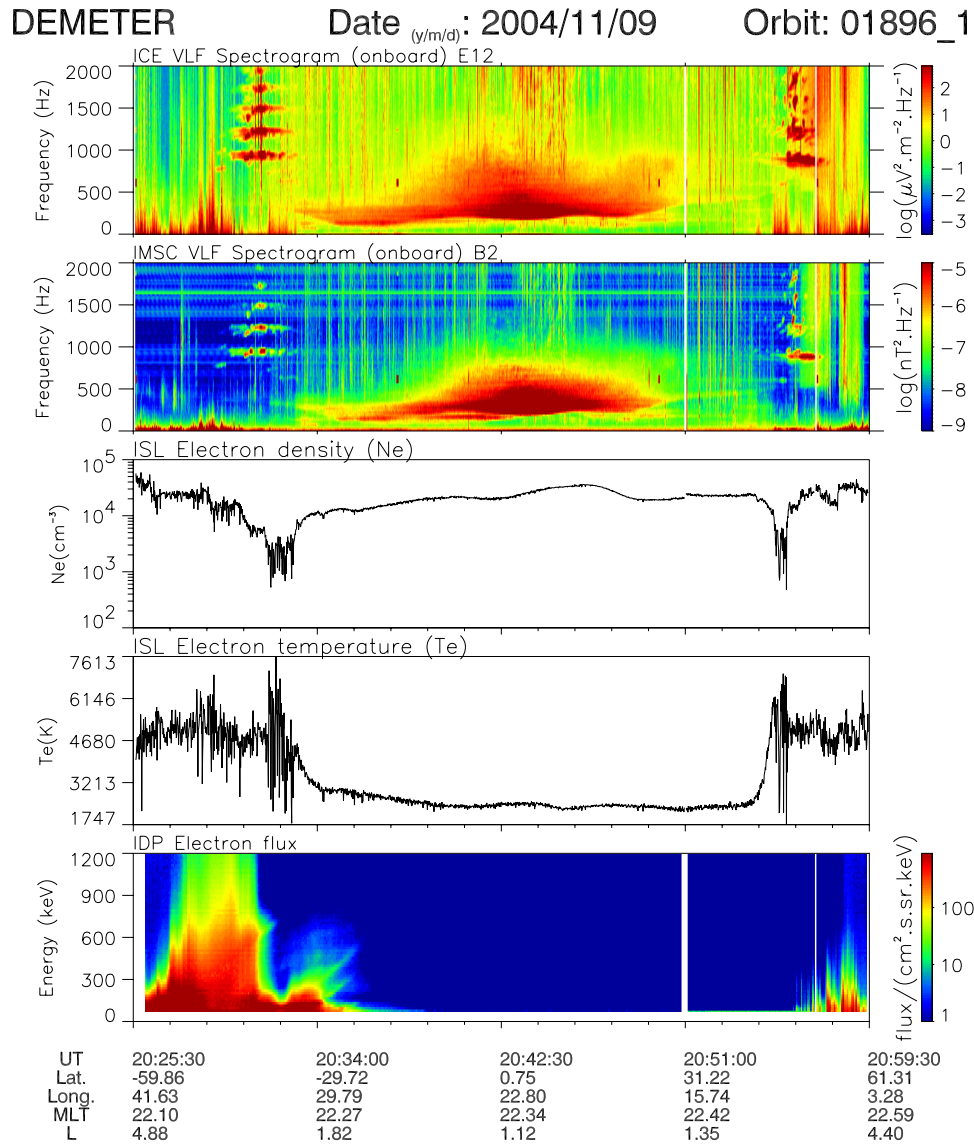


Figure 3. Same as Figure 1 but for data recorded during the up-going half-orbit 1896 on 9 November 2004. The white vertical lines in the spectrograms delimit the time interval where a burst mode is triggered.

emissions are now observed on each side of the equator around 2031:00 UT and 2056:00 UT (nighttime). They appear to be magnetically conjugated because they are both at an L value equal to ~ 2.3 . They have harmonic structures and their frequency bands are centered on 942, 1223, 1482, 1719, and 1935 Hz in the Southern Hemisphere. It corresponds to an averaged frequency spacing of 250 Hz. The maximum intensities of these electric and magnetic spectrograms are $7.9 \times 10^4 \mu\text{V}^2 \text{m}^{-2} \text{Hz}^{-1}$ and $6.9 \times 10^{-5} \text{nT}^2 \text{Hz}^{-1}$, respectively. There is a burst mode between 2051:00 UT and 2057:00 UT, and Figure 4 shows detailed spectrograms of the emission recorded around 2056:00 UT. The top panel is devoted to the electric component and the bottom panel to the magnetic component. Each of the frequency bands appears in fact composed of several spectral lines which display a slow frequency drift in time. Figure 5 shows data recorded during the next half-orbit which is now during

daytime. From the top to the bottom, electric spectrogram, magnetic spectrogram, and electron flux are displayed for one part of the half-orbit because the emissions are only seen around 2143:00 UT. Their maximum intensities are $7.9 \times 10^4 \mu\text{V}^2 \text{m}^{-2} \text{Hz}^{-1}$ and $7.2 \times 10^{-5} \text{nT}^2 \text{Hz}^{-1}$, respectively. As it corresponds to a burst mode a detailed spectral analysis is shown on Figure 6. In this case no frequency splitting is observed. Figure 7 presents another aspect of these bursty emissions. The displayed data are similar to those shown in Figures 1 and 3 but they have been recorded during the second magnetic storm on 21 January 2005 during a daytime half-orbit. The emissions appear at magnetically conjugated locations ($L = \sim 2.6$) around 2012:00 UT and 2038:00 UT. They are simultaneously composed of patchy elements and clear harmonic structures at higher frequencies centered on 1266, 1417, 1547, and 1669 Hz.

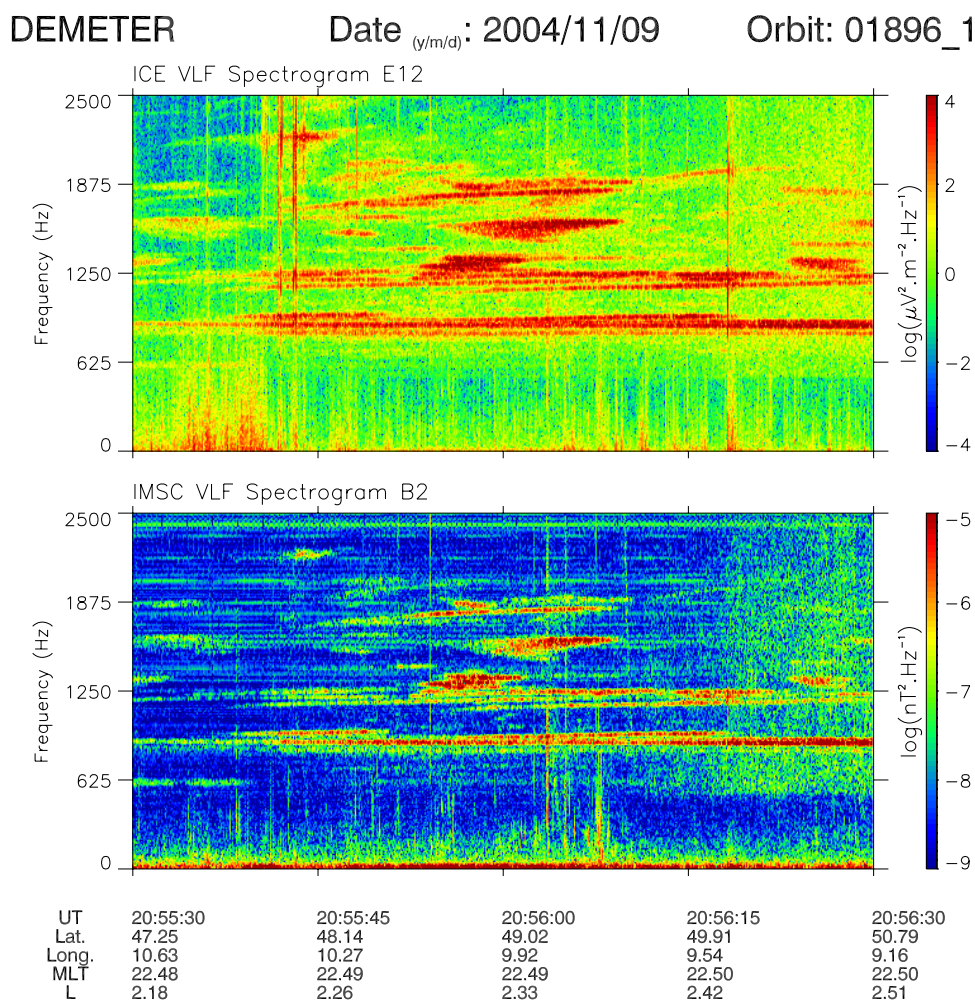


Figure 4. Detailed (top) electric and (bottom) magnetic spectrograms from Figure 3 calculated when the wave experiments were in burst mode. They correspond to 1 min of data, and the frequency range is between 0 and 2.5 kHz.

Then the averaged frequency spacing is 134 Hz. A last representation of these emissions is shown in Figures 8 and 9 which are similar to Figures 1, 3, and 7. Figure 8 corresponds to data recorded on 22 January 2005 during nighttime. Time-modulated harmonic structures are shown around 0017:00 UT. The same kind of structures is also shown around 1013:00 UT at $L = \sim 1.9\text{--}2.3$ in Figure 9 which displays data recorded on 15 May 2005 (the third storm) during daytime. Moreover, the same frequency pattern can be distinguished in Figure 9 at two other times (0955:00 and 1003:00 UT). These two similar frequency patterns appear at conjugated locations ($L = \sim 1.2$) around the magnetic equator, but waves have lower intensities than those observed around 1013:00 UT. In Figures 8 and 9, the frequency of the wave modulation is approximately 35 s.

[7] The observed maximum intensities of the magnetic field fluctuations for the events are between 10^{-5} and 10^{-4} $\text{nT}^2 \text{ Hz}^{-1}$. The maximum intensity of the electric field fluctuations varied approximately between 10^{-8} and 10^{-7} $\text{V}^2 \text{ m}^{-2} \text{ Hz}^{-1}$. These electric and magnetic field intensities are comparable to the strongest emissions of electromagnetic waves at frequencies from a few

hundreds of hertz to a few kHz which can be observed in the Earth's magnetosphere. At altitudes of a few Earth radii, similar intensities were observed in cases of strong equatorial noise or chorus emissions [Santolik *et al.*, 2004, 2005].

4. Wave Analysis

[8] It is possible to determine the propagation characteristics of the observed waves during a burst mode. The six components of the electromagnetic field are therefore available and a relevant software named PRASSADCO has been employed [Santolik, 2001]. A preliminary version of this software has been used to process the data of the FREJA wave experiment [Santolik and Parrot, 1999]. However, it was specially developed for the data analysis of the spectral matrices computed by the STAFF experiment onboard CLUSTER [see, e.g., Santolik *et al.*, 2002a; Parrot *et al.*, 2003], and it has been adapted to process the DEMETER data [Santolik *et al.*, 2006].

[9] The Figures 10 and 11 are related to the wave propagation analysis of two burst mode data sets recorded during these magnetic storms. They all contain the same information. Frequency-time spectrograms of the electric

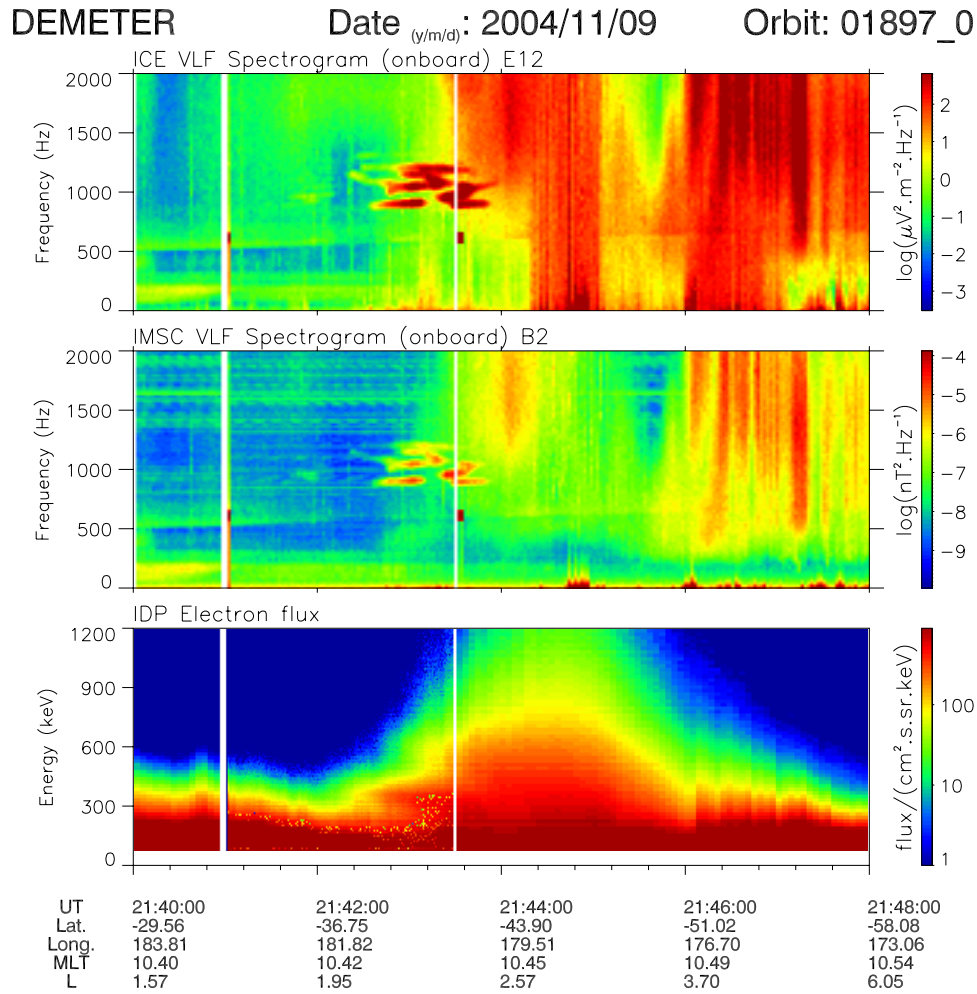


Figure 5. Data recorded during the down-going half-orbit 1897 on 9 November 2004. (top to bottom) VLF spectrogram of one electric component, VLF spectrogram of one magnetic component, and energetic electron flux. The white vertical lines in the spectrograms delimit the time interval where a burst mode is triggered.

and magnetic field fluctuations are shown in Figures 10a, 11a, 10b and 11b. Figures 10c and 11c represent the ellipticity (ratio of the axes of the polarization ellipse) calculated from the magnetic field polarization data using the Singular Value Decomposition (SVD) method [Santolik *et al.*, 2003]. Sign of the result is used to show information on the sense of polarization with respect to the stationary magnetic field: Negative values are used for left-handed polarization sense and positive values for the right-handed polarization sense. The same SVD method is also used to calculate the two angles representing the direction of the wave vector. Figures 10d and 11d show the polar angle θ defined as the angle between the Earth's magnetic field taken as the Z axis and the wave vector. Figures 10e and 11e represent the azimuth angle φ in the plane perpendicular to the Earth's magnetic field with the reference X axis in the magnetic meridian plane and directed away from the Earth.

[10] In the two cases, the ellipticity of the strong structured electromagnetic emissions fluctuates around zero value (linear polarization), with occasional excursions to both negative and positive values. It has been shown [Santolik *et al.*, 2002b] that similar excursions can still be

consistent with the linear polarization, taking into account a possible superposition of waves with different propagation directions. An important property of the two cases is that the wave vector is always close to perpendicular to the Earth's magnetic field. The azimuth of the wave vector does not show any systematic behavior, and the wave vector can be found in the plane of the local magnetic meridian (Figure 11e) but also perpendicular to this plane (Figure 10e). The wave thus propagates in the same mode as the equatorial noise emissions [see Santolik *et al.*, 2004, and references therein].

5. Discussion

[11] These ELF waves are electromagnetic because both electric and magnetic intensities of the emissions are high. For the two events shown in Figures 3 and 5, the experimental calculation of the refraction index gives a value between 10 and 40 at a frequency equal to 900 Hz and it is relatively in good agreement with the cold plasma theory which gives ~ 40 using the following experimental parameters (proton gyrofrequency = 500 Hz, electron density =

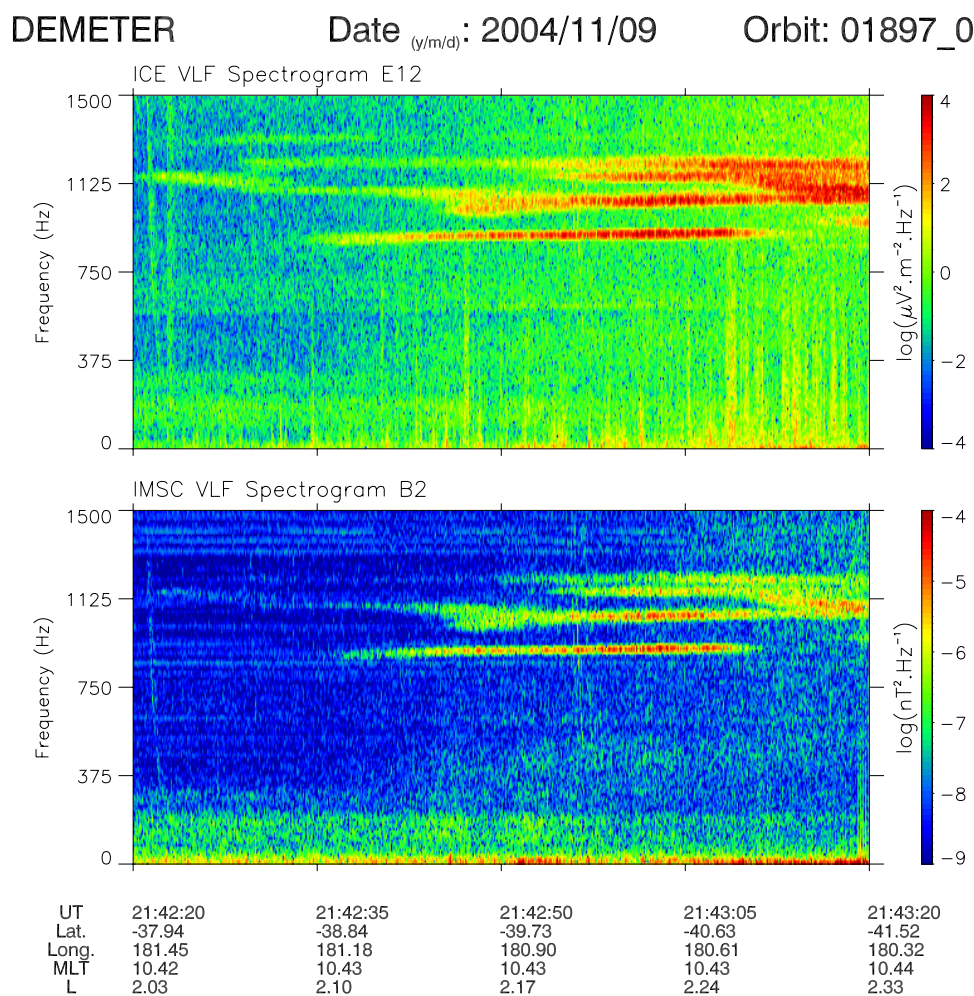


Figure 6. Detailed (top) electric and (bottom) magnetic spectrograms from Figure 5 calculated when the wave experiments were in burst mode. They correspond to 1 min of data, and the frequency range is between 0 and 1.5 kHz.

$2 \cdot 10^4 \text{ cm}^{-3}$, and majority of oxygen ions). The detailed spectral analysis has shown that they are composed of several spectral lines. It can be also seen that the wave elements are most of the time organized in clear harmonic structures. For example, the frequency spacing is 250 Hz in Figure 3 and 134 Hz in Figure 7. Past observations have shown that such harmonic structures in the auroral region or in the equatorial region could be related to Electro-Magnetic Ion Cyclotron (EMIC) waves.

[12] These waves are known to be guided by steep density gradients near the plasmopause [Kasahara *et al.*, 1994; Thorne and Horne, 1997; Fraser and Nguyen, 2001]. DEMETER observations seem indeed to indicate that the emissions are detected in association with regions where both a lower electron density and a higher electron temperature are reminiscent of the ionospheric trough known to be linked to the plasmopause at higher altitudes [Yizengaw *et al.*, 2005]. At night (Figures 1, 3, and 8) the waves appear on the poleward border of these regions; during the day (Figures 7 and 9) they seem to be displaced toward the center of these regions although these latter are less sharp than those observed during nighttime.

[13] Owing to these facts it is expected that the waves observed in the ionosphere by DEMETER are linked to EMIC waves at proton cyclotron harmonics similar to the waves observed in the auroral zone by Chaston *et al.* [2002] or Santolik *et al.* [2002b]. However, in the DEMETER events they must originate from the equatorial region. They could be related to the emissions observed in the equatorial region at much larger L values by Perraut *et al.* [1982] or more recently by Santolik *et al.* [2002a], who observed with Cluster harmonic lines at frequencies higher than 9 times the proton gyrofrequency.

[14] Considering the harmonic structure seen in Figure 3, it is assumed that the frequency interval corresponds to the value of the proton gyrofrequency at the generation location in the equatorial plane. The proton gyrofrequency which has been calculated when the harmonic structure is more clear in the Southern Hemisphere at 2031:00 UT is equal to ~ 250 Hz. It corresponds to the value of the proton gyrofrequency at $L = 1.2$ at the equator for the same meridian plane. Figure 12 illustrates this possibility to find the source of the waves. In this figure, magnetic shells at $L = 1.2$ and $L = 2.3$ are indicated and the dashed line represents a part of

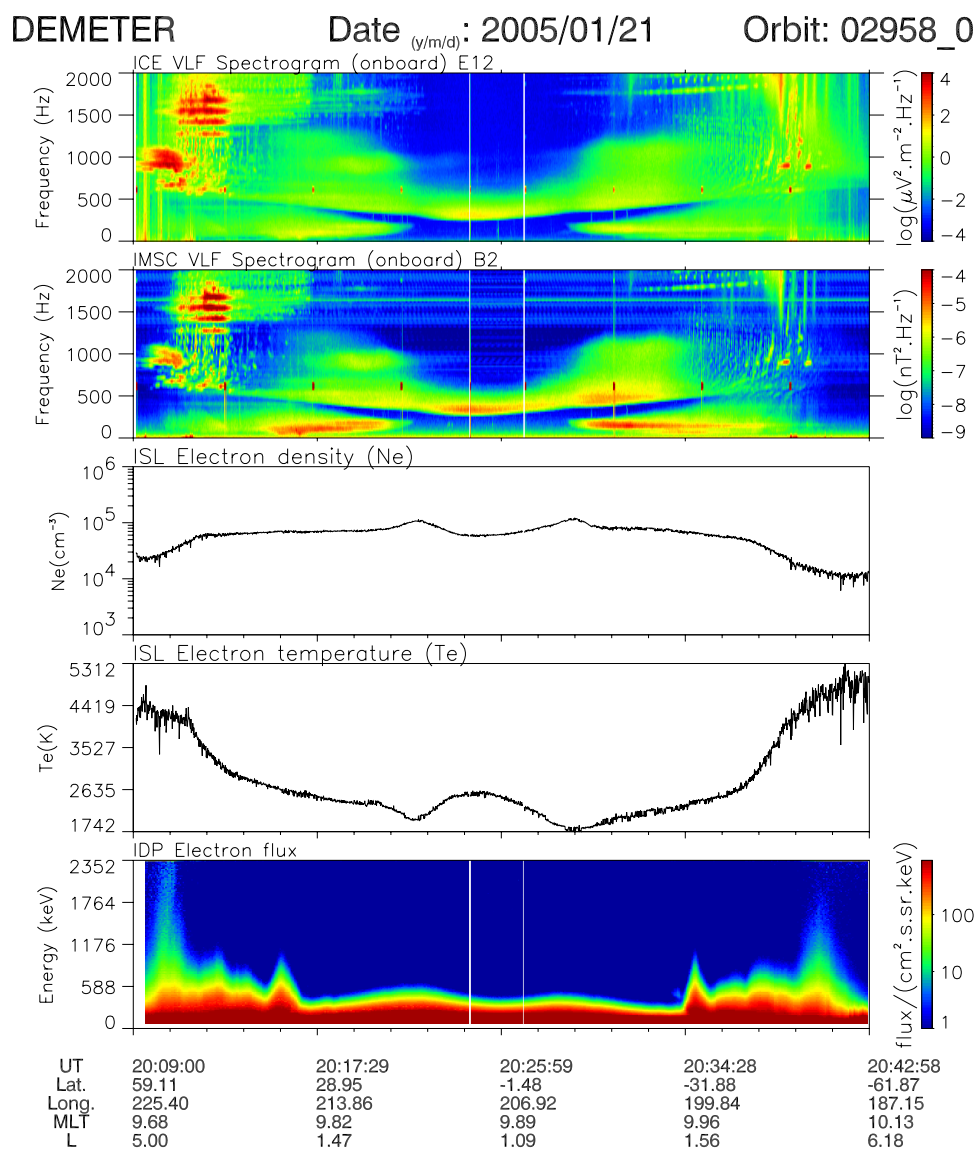


Figure 7. Same as Figures 1 and 3 but for data recorded during the down-going half-orbit 2958 on 21 January 2005.

the satellite orbit. Harmonic waves are emitted at $L = 1.2$ in the equatorial plane. A ray tracing shows that they are bouncing in the magnetosphere toward higher L values. When they find a density gradient which corresponds to the plasmopause location at $L = 2.3$, they propagate down to the ionosphere where they are observed by DEMETER in both hemispheres. The results are similar to a ray tracing study performed by *Sawada et al.* [1991], who have shown that at lower altitudes, waves are reflected back at altitudes when their frequency is equal to the lower hybrid resonance. It is consistent with *Inan and Bell* [1977], who have theoretically shown that waves can be guided in the outer edge of the plasmopause. In such case, these waves have a large polar angle θ at low altitudes as it is observed by DEMETER.

[15] The event shown in Figure 9 where the waves are observed at three different locations is more puzzling.

Owing to the complex structure of the wave elements which are observed around 1013:00 UT, it is more difficult to extract the frequency spacing. A rough estimation gives a value of the proton gyrofrequency equal to ~ 121 Hz which corresponds to a generation zone at $L = \sim 1.5$ in the equatorial plane. Then the satellite observes 3 times the same waves. First after propagation in the magnetosphere, the waves followed the location of the plasmopause at $L = \sim 2.2$ (as it is the case in Figure 12). Second, waves with a weaker intensity are observed close to the generation zone at $L = \sim 1.2$ on each side of the equatorial plane. In this last case it may be presumed that the waves were ducted along the magnetic field line at $L = \sim 1.2$.

[16] The fact that on a given half-orbit, these waves are sometimes observed in one hemisphere (Figures 1, 5 and 8) or in both hemispheres at conjugate points (Figures 3 and 7) can be due to the dimension of the harmonic wave source in

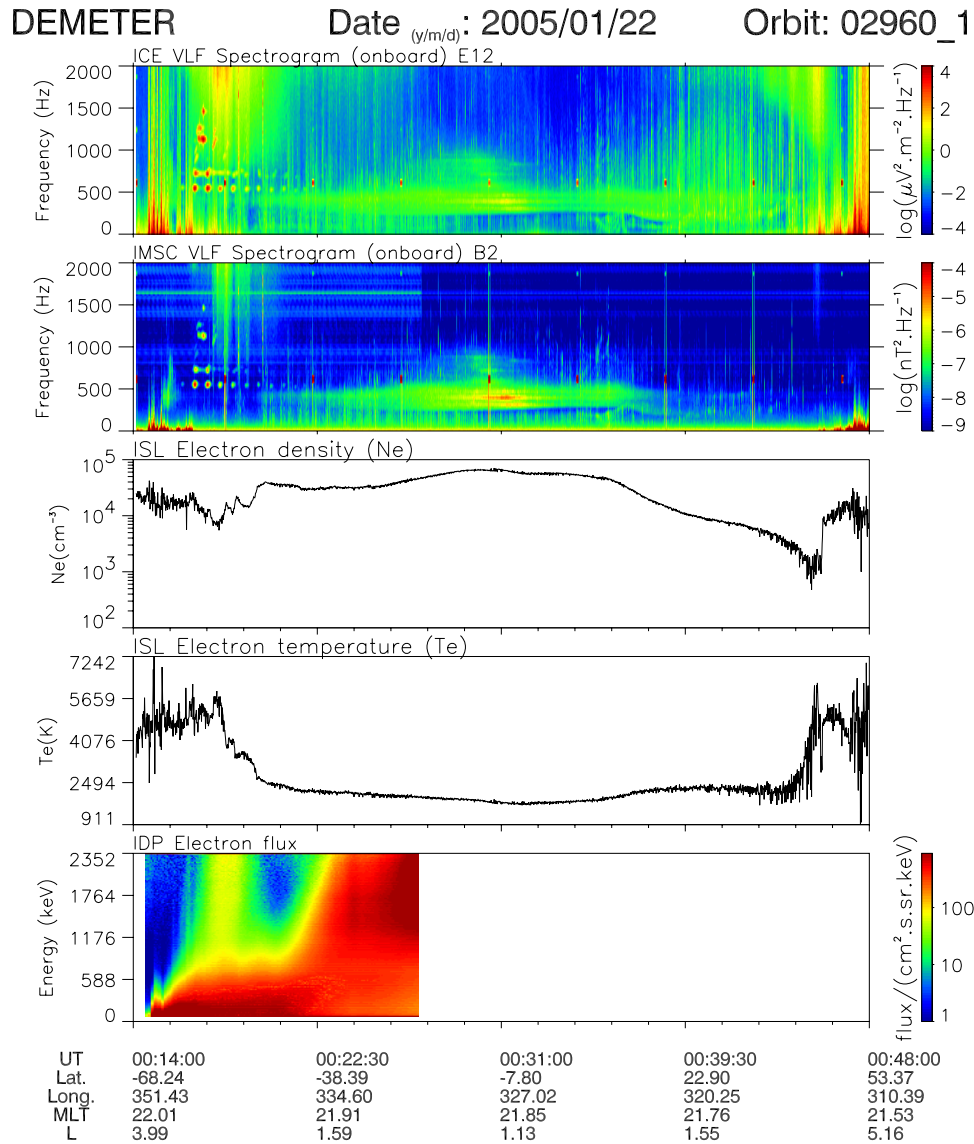


Figure 8. Same as Figures 1, 3, and 7 but for data recorded during the up-going half-orbit 2960 on 22 January 2005.

the equatorial plane. If the source is not enough elongated in longitude, the satellite will observe the waves only in one hemisphere and it will miss their conjugate counterpart owing to the displacement of its orbit in longitude when it will arrive in the other hemisphere.

[17] Even when a harmonic structure is apparent, detailed analysis indicates that in fact many individual spectral lines are present. Why are so many lines observed far from the source region? It is tempting to associate such a frequency splitting with the observations that have been reported in many papers dealing with VLF transmitter signals in the ionosphere. This problem is related to apparitions of sidebands which are sometimes detected during propagation of coherent VLF waves [see, e.g., *Brinca, 1972; Matthews et al., 1984; Bell, 1985; Nunn, 1986; Bell and Ngo, 1988; Lagoutte et al., 1989; Shklyar et al., 1992*, and references therein]. As in the case of VLF transmitter waves, the generation mechanism of sidebands in our events may be due to the scattering from ionospheric irregularities which

are known to be largely enhanced in periods of high magnetic activity.

[18] In Figures 8 and 9, the emissions are time modulated with a period of ~ 35 s which corresponds to the period of Pc3 pulsations. The presence of such pulsations cannot be revealed with the DEMETER data but the modulation of EMIC waves by Pc3 has been already observed by *Rasinkangas and Mursula [1998]*.

[19] Looking at the bottom panels of Figures 2 and 5, it is seen that mirroring electron flux at particular energies can be observed in association with the harmonic ELF emissions observed by DEMETER. Enhancement of relativistic electron flux is known to occur owing to interaction with these waves. The cyclotron resonant equation between relativistic particles of velocity v_R and waves of angular frequency ω and wave vector k can be written as

$$\gamma(\omega - kv_R) - \omega_c = 0, \quad (1)$$

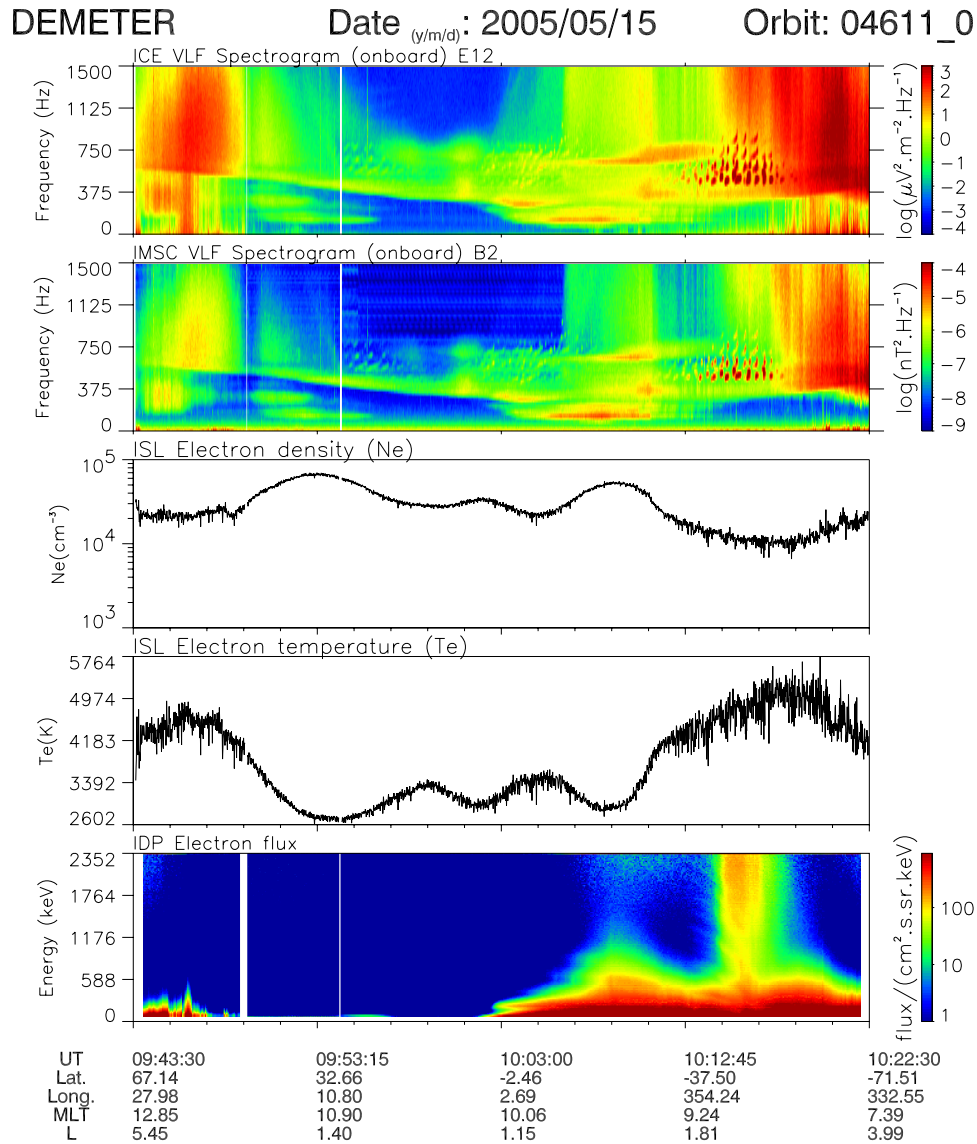


Figure 9. Same as Figures 1, 3, 7, and 8 but for data recorded during the down-going half-orbit 4611 on 15 May 2005.

where ω_e is the electron gyrofrequency and γ is the relativistic factor defined as

$$\gamma = \left(1 - \frac{v_R^2}{c^2}\right)^{-1/2}, \quad (2)$$

where c is the light velocity. The kinetic energy of a particle is

$$E = mc^2(\gamma - 1), \quad (3)$$

where mc^2 is the rest energy of the particle (511 keV for electrons). Equations (1) and (3) have been combined with the dispersion relation in order to obtain the parallel relativistic minimum energy E_R of an electron in resonance with whistler mode wave at the equator. Good agreements have been found: (1) in the example of Figure 2, at 0655:52 UT, the pitch angle is $\sim 78^\circ$ and for a frequency $\omega/2\pi = 957$ Hz ($L = 1.98$) the corresponding energy is $E_R =$

231 keV and the enhancement of the electron flux seen in the last panel is at 197 keV, (2) in the event of Figure 5, at 2142:49 UT, the pitch angle is $\sim 94^\circ$, and for a frequency $\omega/2\pi = 918$ Hz ($L = 2.16$), $E_R = 164$ keV and the measured energy is 171 keV. More details about this wave-particle interaction will be given in a forthcoming paper where it is shown that the value of the wave normal angle with the Earth's magnetic field has a weak influence on the results.

6. Conclusions

[20] New observation of ELF harmonic waves has been performed by the DEMETER microsatellite in the ionosphere. To summarize, the main characteristics of these emissions are the following.

[21] 1. These intense EM waves are only observed during large magnetic storms at frequencies between 500 Hz and 2 kHz. However, it must be noted that they were not present during the 24 August 2005 storm ($Dst = -219$ nT, $K_p = 9-$).

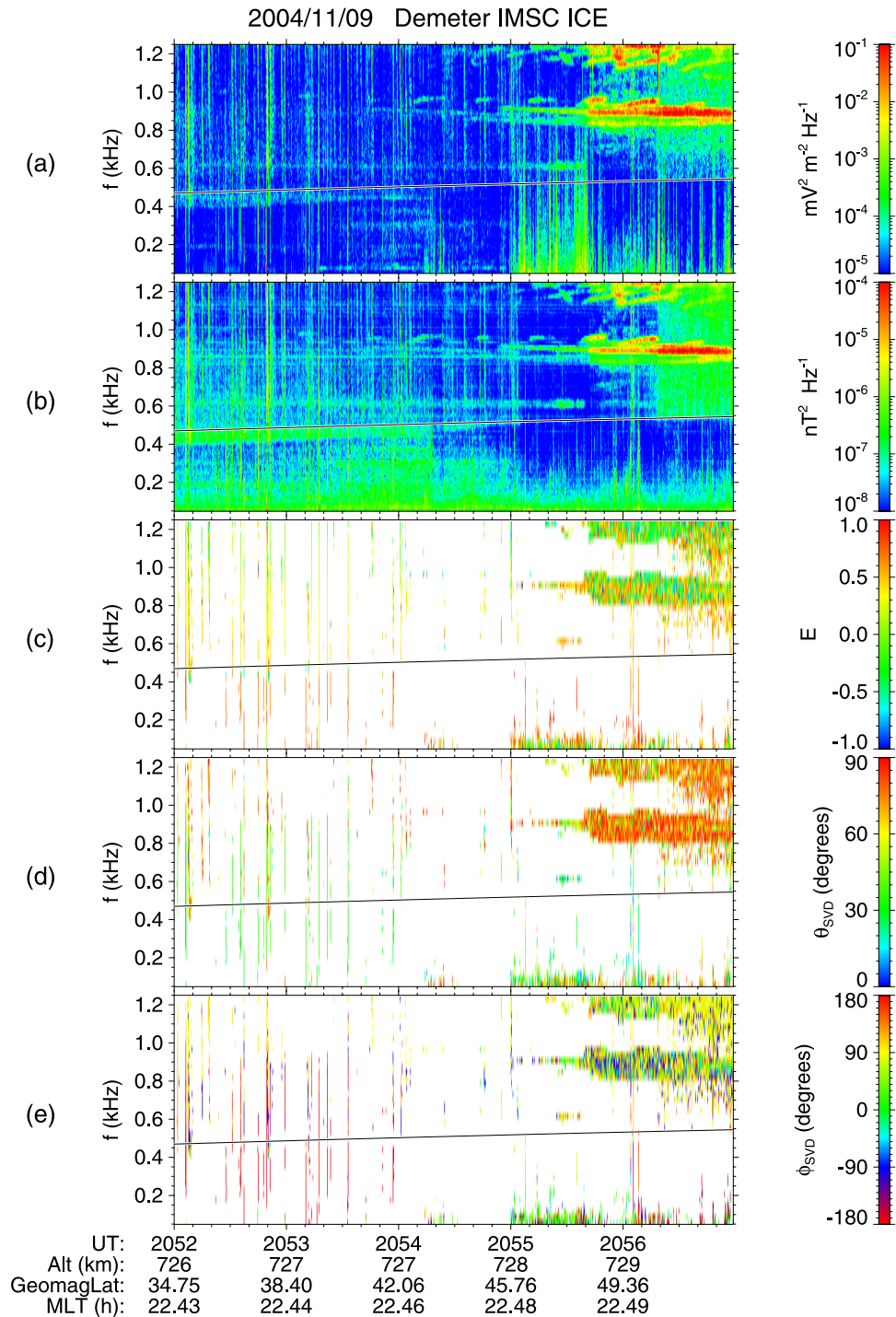


Figure 10. Wave analysis of the burst mode data recorded on 9 November 2004 between 2052 and 2057 UT (see Figure 3). Spectrograms of the (a) electric and (b) magnetic field fluctuations. (c) Ellipticity. (d) Polar angle θ and (e) azimuth angle φ (see text for explanation).

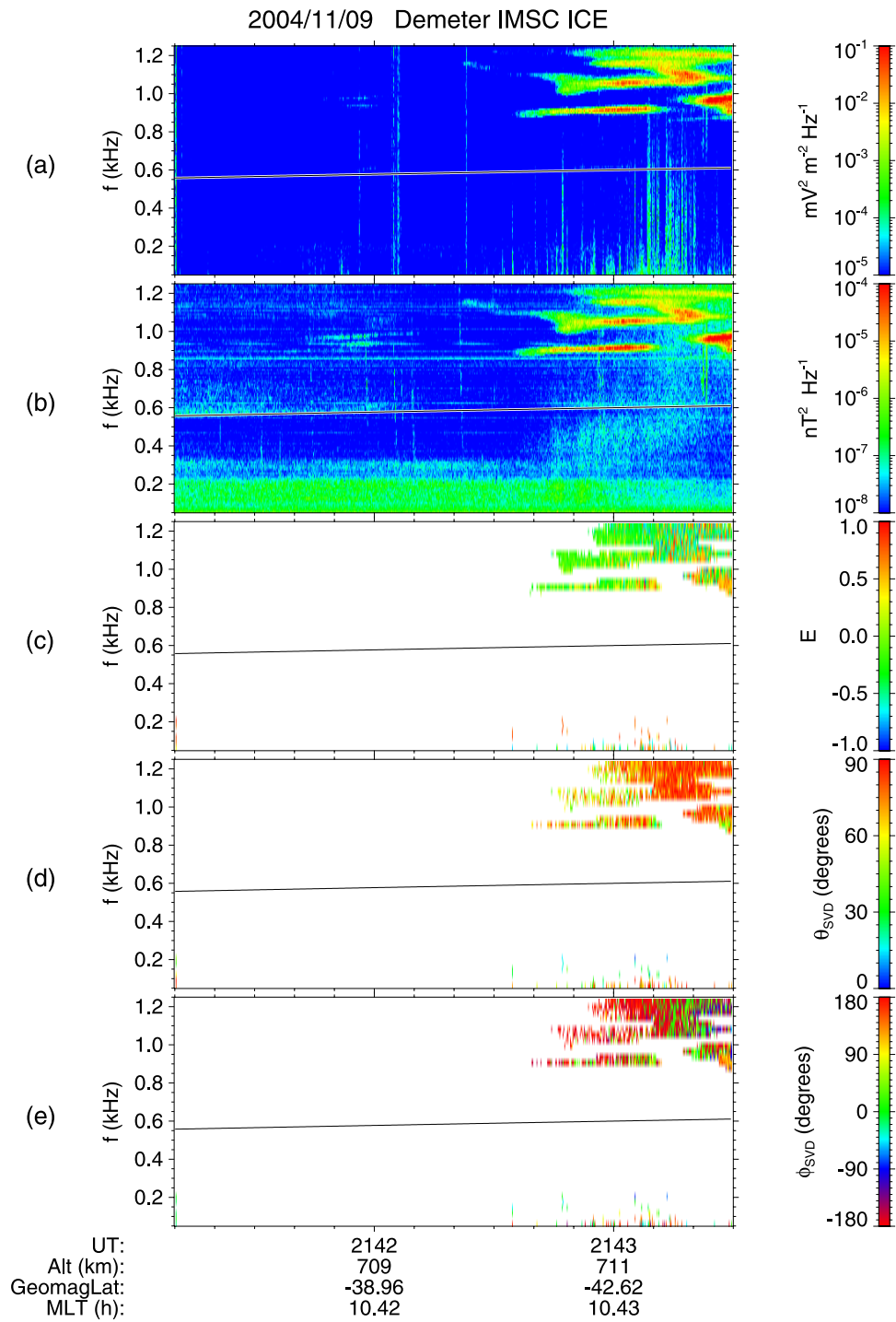


Figure 11. Same as Figure 10 but for the data recorded on 9 November 2004 between 2141.00 and 2143.30 UT (see Figure 5).

DEMETER Date: 2004/11/09 Orbit: 01896_1

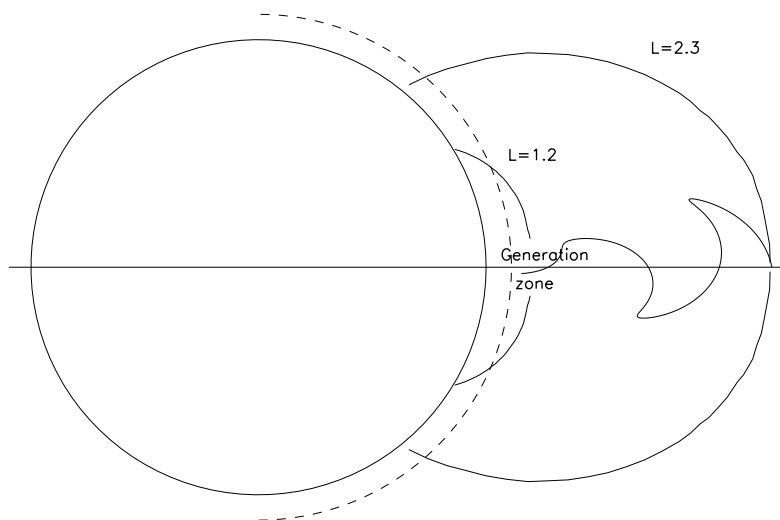


Figure 12. Generation zone of the EMIC waves on 9 November 2004 at $L = 1.2$ in the equatorial region and location of the DEMETER observations of the unstructured waves at $L = 2.3$ in both hemispheres. The dashed circle represents the half-orbit 1896_1 which is up-going. The trace of the ray between $L = 1.2$ and $L = 2.3$ is shown in the meridian plane using a backward ray tracing. The ray calculation starts at $L = 2.3$ for a wave with a frequency equal to 900 Hz and a polar angle θ equal to 85° . A diffusive equilibrium model is used for the electron density.

[22] 2. They are observed in both daytime and nighttime.

[23] 3. It is hypothesized that they are linked to EMIC waves at proton cyclotron harmonics emitted from the equatorial region, bouncing in the magnetosphere and propagating down to the ionosphere because they follow density gradients (plasmopause). In their observation zones they appear to propagate with a direction perpendicular to the magnetic field.

[24] 4. The numerous spectral lines which are observed may be due to scattering from ionospheric irregularities (enhanced by the magnetic activity) during propagation.

[25] 5. During some events, these waves seem to be modulated by Pc3 waves.

[26] 6. They contribute to enhance energetic electron flux.

[27] **Acknowledgments.** The authors thank CNES people involved in the mission development of the DEMETER satellite and those currently in charge of the operations in Toulouse. They are grateful for the support of the DEMETER mission centre engineers (J.-Y. Brochet, D. de Carvalho, and D. Lagoutte) in Orléans. O. S. acknowledges support of the GAAV grant A301120601 and the GACR grant 205/06/1267.

[28] Zuyin Pu thanks both reviewers for their assistance in evaluating this paper.

References

- Bell, T. F. (1985), High-amplitude VLF transmitter signals and associated sidebands observed near the magnetic equatorial plane on the ISEE 1 satellite, *J. Geophys. Res.*, *90*, 2792–2806.
- Bell, T. F., and H. D. Ngo (1988), Electrostatic waves stimulated by coherent VLF signals propagating in and near the inner radiation belt, *J. Geophys. Res.*, *93*, 2599–2618.
- Berthelier, J. J., et al. (2006a), ICE, The electric field experiment on DEMETER, *Planet. Space Sci.*, *54*, 456–471, doi:10.1026/j.pss.2005.10.016.
- Berthelier, J. J., M. Godefroy, F. Leblanc, E. Seran, D. Peschard, P. Gilbert, and J. Artru (2006b), IAP, the thermal plasma analyzer on DEMETER, *Planet. Space Sci.*, *54*, 487–501, doi:10.1016/j.pss.2005.10.018.
- Brinca, A. L. (1972), Whistler side-band growth due to nonlinear wave-particle interaction, *J. Geophys. Res.*, *77*, 3508–3523.
- Chaston, C. C., J. W. Bonnell, J. P. McFadden, R. E. Ergun, and C. W. Carlson (2002), Electromagnetic ion cyclotron waves at proton cyclotron harmonics, *J. Geophys. Res.*, *107*(A11), 1351, doi:10.1029/2001JA900141.
- Cussac, T., M. A. Clair, P. Ultré-Guerard, F. Buisson, G. Lassalle-Balier, M. Ledu, C. Elisabelar, X. Passot, and N. Rey (2006), The DEMETER microsatellite and ground segment, *Planet. Space Sci.*, *54*, 413–427, doi:10.1016/j.pss.2005.10.013.
- Fraser, B. J., and T. S. Nguyen (2001), Is the plasmopause a preferred source region of electromagnetic ion cyclotron waves in the magnetosphere?, *J. Atmos. Sol. Terr. Phys.*, *63*, 1225–1247.
- Gurnett, D. A. (1976), Plasma wave interaction with energetic ions near the magnetic equator, *J. Geophys. Res.*, *81*, 2765–2770.
- Hamrin, M., P. Norqvist, M. André, and A. I. Eriksson (2002), A statistical study of wave properties and electron density at 1700 km in the auroral region, *J. Geophys. Res.*, *107*(A8), 1204, doi:10.1029/2001JA900144.
- Inan, U. S., and T. F. Bell (1977), The plasmopause as a VLF wave guide, *J. Geophys. Res.*, *82*, 2819–2827.
- Kasahara, Y., H. Kenmochi, and I. Kimura (1994), Propagation characteristics of the ELF emissions observed by the satellite Akebono in the magnetic equatorial region, *Radio Sci.*, *29*(4), 751–767.
- Kintner, P. A., and D. A. Gurnett (1977), Observations of ion cyclotron waves within the plasmasphere by Hawkeye 1, *J. Geophys. Res.*, *82*, 2314–2318.
- Kintner, P. M., M. C. Kelley, R. D. Sharp, A. G. Ghielmetti, M. Temerin, C. Cattell, P. F. Mizera, and J. F. Fennell (1979), Simultaneous observations of energetic (keV) upstreaming and electrostatic hydrogen cyclotron waves, *J. Geophys. Res.*, *84*, 7201–7212.
- Lagoutte, D., F. Lefeuvre, and J. Hanasz (1989), Application of bicoherence analysis in study of wave interactions in space plasma, *J. Geophys. Res.*, *94*, 435–442.
- Lagoutte, D., et al. (2006), The DEMETER science mission centre, *Planet. Space Sci.*, *54*, 428–440, doi:10.1016/j.pss.2005.10.014.
- Lebreton, J. P., et al. (2006), The ISL Langmuir Probe experiment and its data processing onboard DEMETER: Scientific objectives, description and first results, *Planet. Space Sci.*, *54*, 472–486, doi:10.1016/j.pss.2005.10.017.
- Liu, H., S. Kokubun, and K. Hayashi (1994), Equatorial electromagnetic emission with discrete spectra near harmonics of oxygen gyrofrequency during magnetic storms, *Geophys. Res. Lett.*, *21*(3), 225–228.

- Lorentzen, K. R., M. P. McCarthy, G. K. Parks, J. E. Foat, R. M. Millan, D. M. Smith, R. P. Lin, and J. P. Treilhou (2000), Precipitation of relativistic electrons by interaction with electromagnetic ion cyclotron waves, *J. Geophys. Res.*, *105*, 5381–5389.
- Matthews, J. P., Y. Omura, and H. Matsumoto (1984), Some PLHR phenomena and their explanation, paper presented at International Wrocław Symposium on Electromagnetic compatibility, Tech. Univ. of Wrocław, Wrocław, Poland.
- Meredith, N. P., R. M. Thorne, R. B. Horne, D. Summers, B. J. Fraser, and R. R. Anderson (2003), Statistical analysis of relativistic electron energies for cyclotron resonance with EMIC waves observed on CRRES, *J. Geophys. Res.*, *108*(A6), 1250, doi:10.1029/2002JA009700.
- Mouikis, C. G., et al. (2002), Equator-S observations of He⁺ energization by EMIC waves in the dawnside equatorial magnetosphere, *Geophys. Res. Lett.*, *29*(10), 1432, doi:10.1029/2001GL013899.
- Nunn, D. (1986), A nonlinear theory of sideband stability in ducted whistler mode waves, *Planet. Space Sci.*, *34*, 429–451.
- Parrot, M., O. Santolík, N. Cornilleau-Wehrin, M. Maksimovic, and C. C. Harvey (2003), Source location of chorus emissions observed by Cluster, *Ann. Geophys.*, *21*, 473–480.
- Parrot, M., et al. (2006), The magnetic field experiment IMSC and its data processing onboard DEMETER: Scientific objectives, description and first results, *Planet. Space Sci.*, *54*, 441–455, doi:10.1016/j.pss.2005.10.015.
- Perraut, S., A. Roux, P. Robert, R. Gendrin, J.-A. Sauvaud, J.-M. Bosqued, G. Kremser, and A. Korth (1982), A systematic study of ULF waves above FH⁺ from GEOS 1 and 2 measurements and their relationships with proton ring distributions, *J. Geophys. Res.*, *87*, 6219–6236.
- Rasinkangas, R., and K. Mursula (1998), Modulation of magnetospheric EMIC waves by Pc3 pulsations of upstream origin, *Geophys. Res. Lett.*, *25*(6), 869–872.
- Russell, C. T., R. E. Holzer, and E. Smith (1970), OGO3 observations of ELF noise, *J. Geophys. Res.*, *75*, 755–768.
- Santolík, O. (2001), Propagation analysis of Staff-SA data with coherency tests, *LPCE/NTS/073.C*, Lab. de Phys. et Chim. l'Environ., CNRS, Orléans, France.
- Santolík, O., and M. Parrot (1999), Case studies on the wave propagation and polarization of ELF emissions observed by Freja around the local proton gyrofrequency, *J. Geophys. Res.*, *104*, 2459–2475.
- Santolík, O., J. S. Pickett, D. A. Gurnett, M. Maksimovic, and N. Cornilleau-Wehrin (2002a), Spatiotemporal variability and propagation of equatorial noise observed by Cluster, *J. Geophys. Res.*, *107*(A12), 1495, doi:10.1029/2001JA009159.
- Santolík, O., J. S. Pickett, D. A. Gurnett, and L. R. O. Storey (2002b), Magnetic component of narrow-band ion cyclotron waves in the auroral zone, *J. Geophys. Res.*, *107*(A12), 1444, doi:10.1029/2001JA000146.
- Santolík, O., M. Parrot, and F. Lefeuvre (2003), Singular value decomposition methods for wave propagation analysis, *Radio Sci.*, *38*(1), 1010, doi:10.1029/2000RS002523.
- Santolík, O., F. Nemeč, K. Gereova, E. Macusova, Y. de Conchy, and N. Cornilleau-Wehrin (2004), Systematic analysis of equatorial noise below the lower hybrid frequency, *Ann. Geophys.*, *22*, 2587–2595.
- Santolík, O., E. Macusova, K. H. Yearby, N. Cornilleau-Wehrin, and H. St. K. Alleyne (2005), Radial variation of whistler-mode chorus: First results from the STAFF/DWP instrument onboard the Double Star TC 1 spacecraft, *Ann. Geophys.*, *23*, 2937–2942.
- Santolík, O., F. Nemeč, M. Parrot, D. Lagoutte, and L. Madrias (2006), Analysis methods for multi-component wave measurements on board the DEMETER spacecraft, *Planet. Space Sci.*, *54*, 512–527, doi:10.1016/j.pss.2005.10.020.
- Sauvaud, J. A., T. Moreau, R. Maggiolo, J. P. Treilhou, C. Jacquey, A. Cros, J. Coutelier, J. Rouzaud, E. Penou, and M. Gangloff (2006), High energy electron detection onboard DEMETER: The IDP spectrometer, description and first results on the inner belt, *Planet. Space Sci.*, *54*, 502–511, doi:10.1016/j.pss.2005.10.019.
- Sawada, A., Y. Kasahara, M. Yamamoto, I. Kimura, S. Kokobun, and K. Hayashi (1991), ELF emissions observed by the Exos-D satellite around the geomagnetic equatorial region, *Geophys. Res. Lett.*, *18*(2), 317–320.
- Shklyar, D. R., D. Nunn, A. J. Smith, and S. S. Sazhin (1992), An investigation into the nonlinear frequency shift in magnetospherically propagated VLF pulses, *J. Geophys. Res.*, *97*, 19,389–19,402.
- Summers, D., and R. M. Thorne (2003), Relativistic electron pitch-angle scattering by electromagnetic ion cyclotron waves during geomagnetic storms, *J. Geophys. Res.*, *108*(A4), 1143, doi:10.1029/2002JA009489.
- Temerin, M., and R. L. Lysak (1984), Electromagnetic ion cyclotron mode (ELF) waves generated by auroral electron precipitation, *J. Geophys. Res.*, *89*, 2849–2859.
- Thorne, R. M., and R. B. Horne (1997), Modulation of electromagnetic ion cyclotron instability due to the interaction with ring current O⁺ during magnetic storms, *J. Geophys. Res.*, *102*, 14,155–14,164.
- Yizengaw, E., H. Wei, M. B. Moldwin, D. Galvan, L. Mandrake, A. Mannucci, and X. Pi (2005), The correlation between mid-latitude trough and the plasmopause, *Geophys. Res. Lett.*, *32*, L10102, doi:10.1029/2005GL022954.
- Young, D. T., S. Perraut, A. Roux, C. de Villedary, R. Gendrin, A. Korth, G. Kremser, and D. Jones (1981), Wave particle interactions near Ω_{He^+} observed on GEOS 1 and 2, 1: Propagation of ion cyclotron waves in He⁺-rich plasma, *J. Geophys. Res.*, *86*, 6755–6772.

J. J. Berthelier, Observatoire de Saint Maur, Centre d'Etude des Environnements Terrestre et Planétaires, Observatoire de Saint Maur, 4 Avenue de Neptune, F-94107 Saint Maur des Fossés, France. (jean-jacques.berthelier@cetp.ipsl.fr)

A. Buzzi and M. Parrot, Laboratoire de Physique et Chimie de l'Environnement, CNRS, 3A, Avenue de la Recherche Scientifique, F-45071 Orléans, France. (buzzi@cnsr-orleans.fr; mparrot@cnsr-orleans.fr)

J. P. Lebreton, Research and Scientific Support Department, ESA/ESTEC, Keplerlaan 1, NL 200 AG Noordwijk, Netherlands. (jean-pierre.lebreton@esa.int)

O. Santolík, Faculty of Mathematics and Physics, Charles University, V. Holešovičkách 2, CZ-18000 Prague 8, Czech Republic. (ondrej.santolik@mff.cuni.cz)

J. A. Sauvaud, Centre d'Etude Spatiale des Rayonnements, CNRS, 9 Avenue du Colonel Roche, F-31028 Toulouse, France. (jean-andre.sauvaud@cesr.fr)